Article

Not peer-reviewed version

Advances in Structural Health Monitoring: Bio-Inspired Optimization Techniques and Vision-Based Monitoring System For Damage Detection Using Natural Frequency

Minkyu Jung , Jiyeon Koo , Andrew Jaeyong Choi *

Posted Date: 10 July 2024

doi: 10.20944/preprints202407.0858.v1

Keywords: Structural Health Monitoring; Bio-inspired Optimization; Video Motion Magnification; Vision-based Damage Detection

 doi:10.20944/preprints202407.0858.v1

Article

Advances in Structural Health Monitoring: Bio-Inspired Optimization Techniques and Vision-Based Monitoring System For Damage Detection Using Natural Frequency

Minkyu Jung, Jiyeon Koo and Andrew Jaeyong Choi *

School of Computing, Dept. of AI-SW, Gachon University, 1342 Seongnam-daero, Sujeong-gu, Seongnam 13306, Republic of Korea
* Correspondence: andrewjchoi@gachon.ac.kr; Tel. +82-31-750-8667

Abstract: This paper introduces the improvements in the natural frequency based Structural Health Monitoring (SHM) by applying bio-inspired optimization methods and the vision-based monitoring system for the effective damage detection. This paper proposes a natural frequency extraction method using the motion magnification based vision monitoring system with bio-inspired optimization techniques to estimate the damage location and depth in a cantilever beam. The proposed optimization techniques are inspired by natural processes and biological evolution including Genetic Algorithms, Particle Swarm Optimization, Sea Lion Optimization, and Coral Reefs Optimization. To verify the performances of each bio-inspired optimization methods, the eigenvalues of a two-bay truss structure are used for estimating the damaged elements. Then, using the proposed video motion magnification method, the natural frequency for each of undamaged and damaged cantilever beam have been extracted and compared with the LDV sensor to verify the proposed vision-based monitoring system. The performance of each bio-inspired optimizer for the damage detection has been compared. As a result, Coral Reefs Optimization has showed the lowest average error, around 1%, in the damage detection using natural frequency.

Keywords: structural health monitoring; bio-inspired optimization; video motion magnification; vision-based damage detection

MSC: 65K10; 68T45;74A45

1. Introduction

1.1. Structural Health Monitoring

Structural Health Monitoring (SHM) associated with potentials for significant safety, reliability, and economic benefits have motivated the need for developing this system. SHM is a technique monitoring dynamic and static properties caused by a damage. The damage can be defined as changes in the properties of material or geometry of a structure that affects the overall performance of the structure.

The most common methods for damage detection are vibration based damage identification methods. The methods can be tested in two different strategies which are model based and non-model based. The model based strategy is comparing a theoretical model with a measured model to identify the damage. The non-model based one is using signal processing algorithms to analyze signal response in time and frequency domains. However, these methods have limitations. It requires expensive devices and is hard to obtain data from a large scale structure. Recently, non-contact methods are introduced such as applying computer vision technology to measure vibration and deformation.

In this paper, a new method of obtaining dynamic data from a structure is proposed. The dynamic data can be used for vision-based techniques. The proposed vision-based monitoring system is performed by using a video motion magnification method to extract natural frequency of cantilever beams. It amplifies the video signal to reveal hidden small motions of the structure.

 doi:10.20944/preprints202407.0858.v1

Furthermore, the optimization technique is used in a wide variety of ways to reduce time and cost to solve problems covered in the structural health monitoring field. In order to monitor the health condition of the structure, there are researches that effectively inspect the fault of the sensor [1] and the optimal sensor placement (OSP) [2–4] in which sensors are placed in the optimal position. In addition, there are researches that applied machine learning to SHM [5,6], that applied traditional optimization techniques to structures [7,8] and that applied novel optimization techniques [9,10]. Novel optimization techniques were inspired by nature and human, respectively, and there are other studies inspired by bio [9,11].

The cantilever beam is a structure with one side fixed and the other in a free form. Due to this structural characteristic, the cantilever beam is widely used for various architectural and engineering purposes, can be the basis of a structure, and a lot of researches have been conducted. Research on cantilever beams [7,12,13] in the context of SHM has demonstrated that damage analysis of structures can be mathematically modeled and transformed into optimization problems. Additionally, these optimization problems can be effectively solved using algorithms, enabling the diagnosis of structural damage.

1.2. Vision-Based Structural Health Monitoring

The vision-based monitoring methods have been extensively applied to SHM to detect damage in a structure. In recent years, vision-based monitoring systems have been widely studied with the development of computers, computing technologies (computer vision, soft computing, etc.) and image sensors (motion capture cameras, high-speed cameras, stereo cameras, etc.) are applied to the SHM field.

Chen et al. [14] identified the modal parameters by measuring cantilever beams and dynamic responses of pipe structures through phase-based motion magnetization methods as a study on the shm field applying computing. Also, there is a study [15] using phase-based motion magnetization with edge detection algorithms and blind source separation to measure the mode shape of building structures and cantilever beams. A stereo camera vision system is used to evaluate and inspect the state of large structures that make up complex structures. It can collect 3D full field images and a study [16] was conducted to obtain the operation shape of wind turbine blades using DIC (Digital Image Correlation) with stereo photogrammetry along with phase-based motion magnetization methods. As such, the vision-based monitoring system is useful in terms of use and cost for inspecting the deformation and vibration of structures. In addition, it is evaluated as a promising technology in the SHM field because it has the potential to measure the overall dynamic responses of the structure.

This paper is an extended work of our previous research [7]. We proposes an innovative SHM system to estimate and detect the damage in a cantilever beam using the vision-based monitoring system with phase-based motion magnification and bio-inspired optimization methods. Our previous work applied a real-value encoding Genetic Algorithm (GA). To improve the results of estimating the damage location and depth on the cantilever beams, different types of bio-inspired optimizers are compared to estimate more accurate locations and depth of the damage on the cantilever beam by optimizing the natural frequencies obtained from the proposed vision-based monitoring system. The overall flowchart of the proposed work is illustrated in Figure 1.

 doi:10.20944/preprints202407.0858.v1

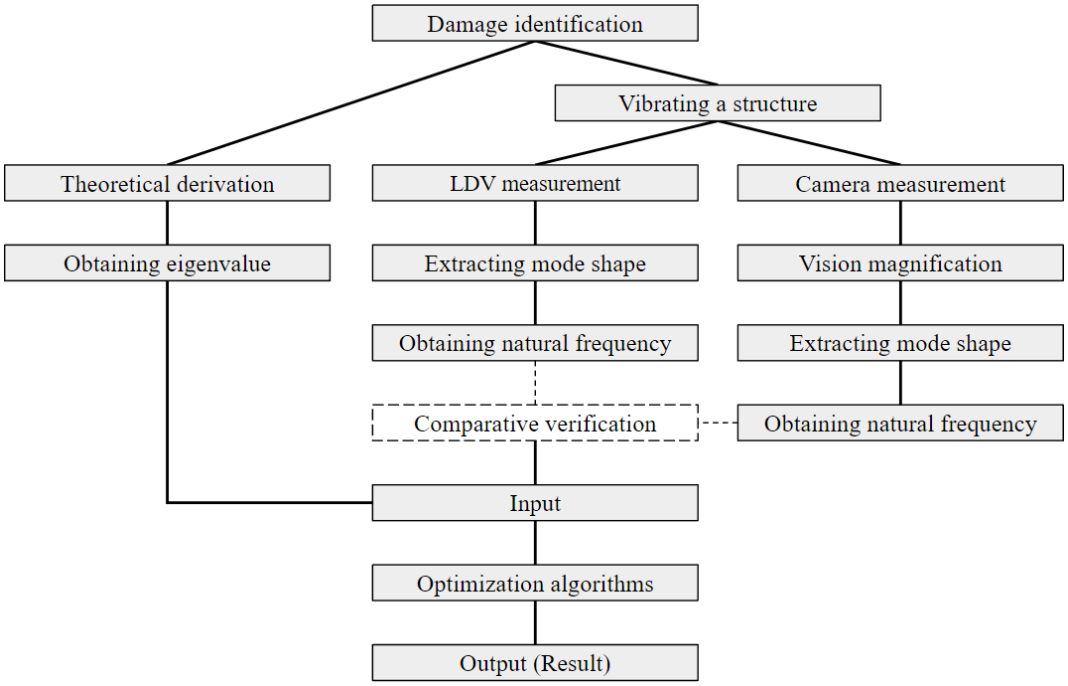

Figure 1. Overall flowchart for vision-based structural health monitoring

2. Overview of Bio-Inspired Optimization

Bio-inspired optimization algorithms are a type of algorithms derived from natural processes and biological evolution. These algorithms utilize mechanisms observed in nature, such as selection, reproduction, mutation, and social behaviors, to find optimal solutions to complex problems. Bio-inspired optimization techniques are extensively applied across diverse fields such as environmental science, finance, engineering, and manufacturing, due to their flexibility and effectiveness in solving multi-dimensional and non-linear optimization problems.

Both swarm-based and evolutionary-based optimization techniques are included in Bio-inspired optimization. Swarm-based optimization algorithms are inspired by the collective action observed in decentralized, self-organizing systems, such as bird flocks or fish schools. In contrast, Evolutionary-based optimization algorithms are inspired by the principles of natural selection and genetic evolution.

In this section, we will discuss several prominent bio-inspired optimization algorithms, such as genetic algorithms, particle swarm optimization, sea lion optimization, and coral reefs optimization. Particle swarm optimization and sea lion optimization fall under the Swarm-based category, while genetic algorithms and coral reefs optimization fall under the Evolutionary-based category. Each of these algorithms mimics a different natural process and has unique characteristics that make it suitable for different types of optimization problems.

2.1. Genetic Algorithm

Genetic algorithms (GA) [17,18], one of the types of evolutionary-based optimization, are a kind of stochastic optimization technique inspired by the principles of natural evolution and heredity. GA performs well in exploring complex optimization problems in parallel and globally, and finding optimal solutions. Applying Darwin's theory of natural selection, it goes through a process where good solutions survive and bad solutions disappear in a set of candidate solutions. GA goes through repetitive search processes to find the optimal solution. In the initialization phase, which is performed once at a time, GA randomly creates a set of individuals called chromosomes. At this time, each entity represents a point in the solution space. After that, GA performs three important actions at each stage that imitate the behavior of the genetics of initialization, selection, crossover, and mutation. Each action mimics the genetic principle as follows.

 doi:10.20944/preprints202407.0858.v1

- Selection: Select an individual from the current group. This is the process of becoming the parent of the next generation, and preferably a good parent should be selected to produce offspring. The selection phase includes the selection of Roulette wheel, Tournament selection, Ranking-based selection, and Elitism. Each method in common increases the likelihood of being transmitted to future generations.
  - In Roulette wheel selection, the chromosomes are compared to each other to select the chromosome to be passed on to the next generation in the current set of objects. In the Roulette wheel selection, the probability of selection for the i-th chromosome is expressed mathematically as $p(x_i) = f(x_i) / \sum_{j=1}^{N} f(x_j)$, where f is the fitness function and N is the number of chromosomes present in a generation.
  - Tournament selection produces a random number between 0 and 1 after randomly selecting two chromosomes. If this value is less than threshold, choose the one with the higher fit, or choose the one with the lower fit.
  - In Ranking-based selection, chromosomes are selected based on ranking rather than fit. Ranking each chromosome in an individual set is done, and the better the ranking, the better the probability of being selected.
  - In Eliteism, Some of the best chromosomes are selected (considering elitism rate β), and the selected chromosomes are passed on to the next generation without any change. This maintains good information and helps improve performance.
- Crossover: The characteristics of the two solutions are crossed and partially combined to create one new characteristic. Methods of crossover include single point, two point, and uniform. The single point and two point mean the number of intersections and combine the characteristics of the two chromosomes based on each intersection. The unit generates a random number at each genetic factor location on the chromosome and intersects the characteristics between the two chromosomes compared to threshold.
- Mutation: In this phase, mutation is applied to some chromosomes probabilistically (considering mutation rate γ) across the entire chromosome. Randomly changing the genetic factors of chromosomes to cause other harm, allowing the children to have features that are not present in the parents. This prevents the entire generation from converging to the local minimum.

 doi:10.20944/preprints202407.0858.v1

Algorithm 1: Genetic Algorithm

Input: Population size α
Elitism rate β
Number of generations δ
Mutation rate γ
Output: Optimal solution X

Initialize the population of size α with random feasible solutions;
Store them in the population Pop;
while *termination condition not satisfied* **do**
  for $i \leftarrow 1$ **to** δ **do**
    $n_e \leftarrow \alpha \cdot \beta$;
    Find the best n_e solutions in Pop and store them in Pop_1;
    $n_c \leftarrow \frac{\alpha - n_e}{2}$;
    for $j \leftarrow 1$ **to** n_c **do**
      Choose two solutions X_A and X_B, randomly from Pop;
      Perform one-point crossover on X_A and X_B to generate new solutions X_C and X_D;
      Add X_C and X_D to Pop_2;
    end
    for $j \leftarrow 1$ **to** n_c **do**
      Find a solution X_j in Pop_2;
      Mutate each bit of X_j with mutation rate γ to create a new solution X'_j;
      if X'_j *is infeasible* **then**
        Repair X'_j to make it feasible;
      end
      Replace X_j in Pop_2 with the new solution X'_j;
    end
    Update Pop $\leftarrow \text{Pop}_1 + \text{Pop}_2$;
  end
end
Return the best solution X in Pop;

2.2. Particle Swarm Optimization

Swarm-based optimization is a type of mathematical optimization in which multiple optimizers exchange information to perform optimization. Compared to single-agent optimization, it requires more computational resources but is more likely to converge to the global optimum. One of the well-known algorithms in optimization inspired by swarm-based is Particle Swarm Optimization (PSO), which was proposed in 1995 [19]. PSO draws inspiration from the social behavior patterns seen in bird flocks and fish schools. The method finds the optimal solution by considering both the individual optimal found in each particle and the global optimal found in the entire swarm. In Heppner's bird simulation [20], the introduction of a two-dimensional *comfield vector* is proposed to model the dynamic behavior of the flock. Each agent within the simulation evaluates its current position (x_i, y_i) using $\sqrt{(x - x_i)^2} + \sqrt{(y - y_i)^2}$ with a value of 0 when the current position is (100, 100).

The optimal solution is determined as Equation (1):

$$v_i(t+1) = v_i(t) + 2 \cdot \text{rand}() \cdot (\text{pBest}_i - x_i(t)) + 2 \cdot \text{rand}() \cdot (\text{gBest} - x_i(t)) \tag{1}$$

where $v_i(t)$ and $x_i(t)$ are velocity and position of particle i at point t, "$pBest_i$ represents the optimal position discovered by particle i to date, while $gBest$ indicates the best position indentified as the

 doi:10.20944/preprints202407.0858.v1

entire swarm. The decision to subtract or add g with a random constant applied to v_i is determined by comparing x_i with $gBest$, where the g is a weight parameter.

$$\mathrm{v}_x \leftarrow \begin{cases} \mathrm{v}_x - \mathrm{rand}() \cdot g & \text{if } \mathrm{X}_x > \mathrm{pBest}_x[\mathrm{gbest}] \\ \mathrm{v}_x + \mathrm{rand}() \cdot g & \text{if } \mathrm{X}_x < \mathrm{pBest}_x[\mathrm{gbest}] \end{cases}$$

$$\mathrm{v}_y \leftarrow \begin{cases} \mathrm{v}_y - \mathrm{rand}() \cdot g & \text{if } \mathrm{X}_y > \mathrm{pBest}_y[\mathrm{gbest}] \\ \mathrm{v}_y + \mathrm{rand}() \cdot g & \text{if } \mathrm{X}_y < \mathrm{pBest}_y[\mathrm{gbest}] \end{cases}$$

Algorithm 2: Particle Swarm Optimization (PSO)

Input: Number of iterations T
Number of particles n
Dimensions of the search space d
Inertia weight ω
Cognitive factor c_1
Social factor c_2

Output: Optimal global position gBest and its corresponding evaluation score

for *one particle i of n* **do**
  Randomly set the particle's initial position x_i within the search space;
  Randomly initialize the particle's velocity v_i;
  Set the individual best position pBest_i to the initial position x_i;
  Calculate the evaluation score $f(\mathrm{pBest}_i)$;
end
Determine the global best position gBest as the position of the particle with the highest evaluation score among all particles;
while $t < T$ **do**
  for *one particle i of n* **do**
    Compute the evaluation score $f(x_i)$;
    if $f(x_i)$ *is superior to the personal best evaluation score* $f(pBest_i)$ **then**
      Update pBest_i to the current position x_i;
    end
  end
  Update gBest to the position of the particle with the highest evaluation score among all particles;
  for *each particle i* **do**
    Revise the particle's velocity v_i by the following equation:;

$$v_i(t+1) = \omega \cdot v_i(t) + c_1 \cdot \mathrm{rand}() \cdot (\mathrm{pBest}_i - x_i(t)) + c_2 \cdot \mathrm{rand}() \cdot (\mathrm{gBest} - x_i(t))$$

    Update the particle's position x_i by the following equation:;

$$x_i(t+1) = x_i(t) + v_i(t+1)$$

  end
  Increment t by 1;
end

 doi:10.20944/preprints202407.0858.v1

2.3. Sea Lion Optimization Algorithm

The Sea Lion Optimization (SLnO) algorithm [21], like PSO, is an optimization method inspired by swarm activity. SLnO is a metaheuristic optimization method modeled after hunting behavior of sea lions. Sea lions utilize their whiskers to recongnize the location of their prey., communicate with each other through vocalizations, and hunt in groups. These behaviors are mathematically modeled as follows to solve optimization problems effectively.

First, in the Detecting and tracking phase:

$$\overrightarrow{D} = |2 \cdot \overrightarrow{B} \cdot \overrightarrow{P(t)} - \overrightarrow{X(t)}| \tag{2}$$

$$\overrightarrow{X(t+1)} = \overrightarrow{P(t)} - \overrightarrow{D} \cdot \overrightarrow{C} \tag{3}$$

equation (2) indicates the distance between the sea lion $\vec{X}$ and the target prey $\overrightarrow{P(t)}$ at point t, where $\vec{B}$ is a random vector in $[0, 1]$, which is multiplied by 2 to expand the solution area and assist in identifying the optimal solution efficiently. Equation (3) represents the process of approaching the target prey, where $\vec{C}$ decreases linearly from 2 to 0.

Second, in the Communication phase, when the sea lions detect prey, they exchange information through vocalization. This behavior is modeled by the following Equation (4) to enhance the algorithm's performance by ensuring that all agents work together to find the optimal solution.

$$V_{\text{leader}} = \left| \frac{V_w(1 + V_a)}{V_a} \right| \tag{4}$$

where V_{leader} is the velocity of sound of the sea lion leader, V_w and V_a are the speeds of sound in water and air, respectively, each having values of $sin\theta$ and $sin\phi$.

Third, the attacking (hunting) phase is crucial for refining the search process and honing in on the optimal solution. This phase involves two main phases: Dwindling encircling technique and Circle updating position. In the Dwindling encircling technique, the gradual encircling of the prey by sea lions is mathematically modeled. In Equation (3), the value of $\vec{C}$ is decreased linearly from 2 to 0, which helps to narrow the search space around the prey. The Circle updating position, where sea lions encircle and attack the prey from all directions, is mathematically modeled as follows in Equation (5).

$$X(t+1) = |P(t) - X(t)| \cdot \cos(2\pi m) + P(t) \tag{5}$$

where m is a random number in $[-1, 1]$, and $\cos(2\pi)$ is used because the sea lions swim along a circular path to hunt the prey.

Fourth, in the Searching for prey phase, the exploration is diversified using a random value $\vec{C}$ to enhance the search for the global optimum. If $\vec{C}$ is smaller than 1, the position of the search agent is updated. If $\vec{C}$ is bigger than 1, a search agent is selected randomly. If the optimal solution is found, the SLnO algorithm ends.

 doi:10.20944/preprints202407.0858.v1

Algorithm 3: Sea Lion Optimization (SLnO) Algorithm

Input: Maximum number of iterations T
Population size n
Initial positions of agents $\vec{X}_i$
Initial velocities of agents $\vec{V}_i$
Output: Optimal solution $\vec{X}$

Randomly initialize sea lion population with positions $\vec{X}_i$ and velocities $\vec{V}_i$;
Choose a random search agent $\vec{X}_{\text{rand}}$;
Evaluate fitness for each agent;
Set $\vec{X}$ to the agent with the highest fitness;
while $t < T$ **do**
    Compute $\vec{V}_{\text{leader}} = \left| \frac{\vec{V}_1(1+\vec{V}_2)}{\vec{V}_2} \right|$;
    if $\vec{V}_{leader} \geq 0.25$ **then**
        if $|\vec{C}| \geq 1$ **then**
            Select a random search agent $\vec{X}_{\text{rand}}$;
            Update position: $\vec{X}(t+1) = \vec{X}_{\text{rand}}(t) - \vec{D} \cdot \vec{C}$;
        end
        else
            Calculate $\vec{D} = \left| 2\vec{B} \cdot \vec{P}(t) - \vec{X}(t) \right|$;
        end
    end
    else
        Update position: $\vec{X}(t+1) = \left| \vec{P}(t) - \vec{X}(t) \right| \cos(2\pi m) + \vec{P}(t)$;
    end
    if *agent is not part of* $\vec{X}_{leader}$ **then**
        Recompute fitness for all agents;
        Update $\vec{X}$ if a superior solution is found;
        return $\vec{X}$ (Optimal solution);
        stop;
    end
    Increment t by 1;
end

2.4. Coral Reefs Optimization Algorithm

The Coral Reefs Optimization (CRO) [22] algorithm is a novel combination of biological inspiration and meta-heuristic algorithm designed to solve complex optimization problems by simulating the natural processes of coral reef development and coral reproduction. Coral reefs, during their growth process, engage in a competitive struggle to occupy available space. This competition, combined with the unique reproductive mechanisms of corals, leads to the development of a robust and efficient optimization algorithm. CRO algorithm models the reef as a grid (Λ) of size $N \times M$. Each grid cell can host a coral (solution) or be empty. The initial proportion of occupied cells is denoted as ρ_0. Each coral has an corresponding health function $f(X_{ij})$ that denotes the objective function value of the optimization problem. CRO algorithm simulates both sexual and asexual reproduction of corals:

- Broadcast Spawning (External Sexual Reproduction): A portion of corals are selected to release gametes into the water. These gametes combine to form larvae that try to settle on the reef.

 doi:10.20944/preprints202407.0858.v1

- Brooding (Internal Sexual Reproduction): A portion of corals reproduce by internal mutation, producing larvae that are released into the water.
- Larvae Setting: Larvae attempt to settle in the reef. When a larva attempts to settle in a cell that is occupied, it replaces the existing coral when its health function has improved. Each larva has a limited number of attempts before being depredated.
- Asexual Reproduction (Budding or Fragmentation): The corals currently present in the reefs are sorted based on their health levels as determined by a certain criterion. A portion of the best corals replicate and attempt to establish themselves in various parts of the reef.
- Depredation in Poly Phase: With a small probability, the worst corals are removed from the reef, freeing up space for new corals.

Algorithm 4: Coral Reefs Optimization (CRO) Algorithm

Input: Matrix dimensions $N \times M$
Maximum iterations T
Initial population size P
Crossover probability F_b
Mutation probability $1 - F_b$
Asexual reproduction portion F_a
Depredation portion F_d

Output: Best solution found

Generate an $N \times M$ coral reef matrix ρ_o
Initialize the reef with a random population of P solutions until the proportion of empty cells is less than 0.4
while $t < T$ **do**
    Broadcast Spawning:
    Select pairs of solutions for crossover with probability F_b
    Perform crossover to generate new solutions
    Brooding:
    Select solutions for mutation with probability $1 - F_b$
    Perform mutation to generate new solutions
    Larvae Setting:
    Place new solutions into empty cells in the reef matrix or replace worse solutions if the new solutions are better
    Asexual Reproduction:
    Clone a proportion F_a of the best solutions to generate new solutions
    Depredation:
    Remove a proportion F_d of the worst solutions to increase the number of empty cells
    if *stop criteria met* **then**
        break
    end
    Increment t by 1
end
Return the best solution found

3. Estimation of Damage Detection in 2-Bay Truss Structure Using Bio-Inspired Optimization Methods

To verify the performances of each bio-inspired optimization methods, the eigenvalues of a two-bay truss structure are used for estimating the damaged elements. A two-bay truss is shown in Figure 2. The numbers in the dotted circle indicate the element numbers and the numbers with red

Preprints.org (www.preprints.org) | NOT PEER-REVIEWED | Posted: 10 July 2024 doi:10.20944/preprints202407.0858.v1

arrows indicates the unconstrained degrees of freedom. To estimate and detect the damage in the truss structure, calculating all 9 unconstrained DOF is not practical and not efficient. Therefore, only the first three unconstrained DOF are used for the damage detection. This two-bay truss structure has nine unconstrained degrees of freedom and each element in the truss have the following characteristics: Young's modulus of elasticity E = 70 GPa (70×109 N/m2), Poisson's ratio = 0.33, mass density = 2700 kg/m3 and cross-sectional area A = 0.01 m2. Three different cases for the truss structure are evaluated: (1) 50% damaged at element 7, (2) damaged 20% at element 10, and (3) 30% damaged at element 3 and 20% damaged at element 8.

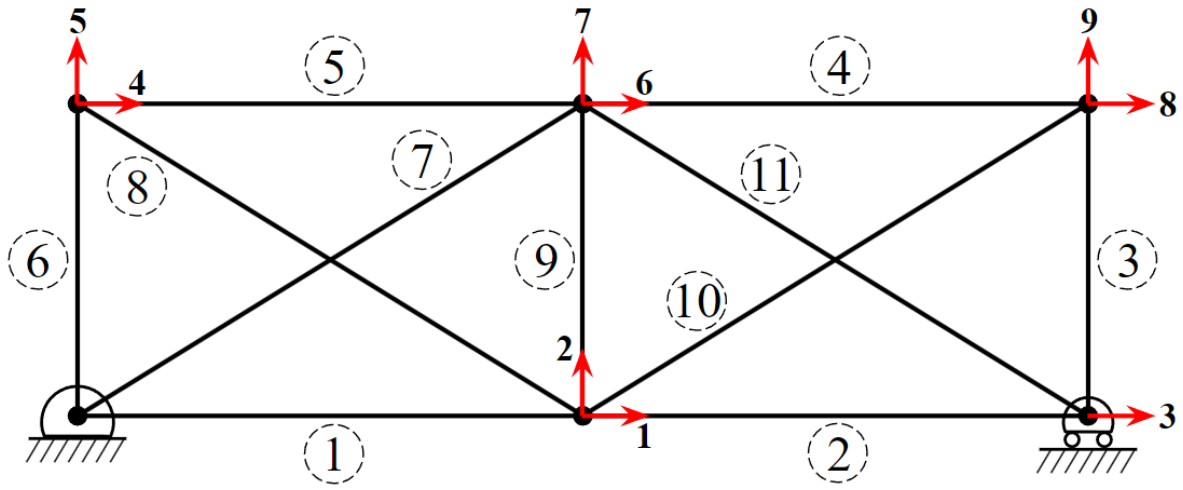

Figure 2. 2-bay truss structure

The Residual Force Method (RFM) is a powerful technique used to update finite element models by reducing the residuals between the predicted and observed results of a structure. RFM specifically aims to adjust the mass and stiffness matrix so that the updated model accurately reflects The dynamic response of the structure subjected to various load conditions. The RFM involves the following steps:

1. Initial Model Analysis: Solve the initial finite element model to get modal properties including natural mode shapes and frequencies.
2. Experimental Data Collection: Measure the structure's dynamic behavior under similar conditions.
3. Residual Calculation: Calculate the residual forces, which are the residuals between the predicted forces and those measured by the initial model.
4. Model Updating: Adjust the parameters of the stiffness matrices and mass stiffness matrices to minimize these residual forces, thereby improving the model's accuracy.

The RFM analysis process for a finite element 2-bay truss structure will be described, including the relevant equations. During the examination of MDOF structural dynamic systems, the equation of motion is a fundamental aspect. This can be expressed as:

$$V(t) = [M]\ddot{z}(t) + [K]z(t) \tag{6}$$

where V is a vector represented by the product of two term, M and K. M is the mass matrix, K is the stiffness matrix, and z is the physical displacement vector. Equation (6) can be rewritten for the j-th eigenvalue equation as Equation (7):

$$[K]\{\Phi_j\} - \lambda_j[M]\{\Phi_j\} = 0 \tag{7}$$

where λ_j is the eigenvalue and $\{\Phi_j\}$ is the eigenvector for the normalized eigenvalue. In the finite element model of the structure, the overall stiffness can be represented as the aggregate of the expanded

 doi:10.20944/preprints202407.0858.v1

stiffness matrices of the individual elements. In the case of the damaged structure, the stiffness matrix is represented the total of element stiffness matrices multiplied by a parameter, and the equation is as follows:

$$[K_d] = \sum_{i=1}^{n} \beta_i [K]_i \tag{8}$$

where n is the total number of elements, $[K]_i$ is the expanded stiffness matrix of the i-th element, and β_i is the reduction parameter of the i-th element and has a value between 0 and 1. 1 means that an element is undamaged, and a value less than 0 or 1 means that it is an element that is either completely or partially damaged. The equation for the eigenvalue used in RFM can be derived from Equation (7) and Equation (8) as follows:

$$\sum_{i=1}^{n} \beta_i [K]_i \Phi_{jd} - \lambda_{jd} [M] \Phi_{jd} = R_j \tag{9}$$

where $[R]$ is the residual force matrix with a size of $n \times m$, where n and m are the number of elements and the number of modes, respectively. For 1^{st} mode, $[R]$ can be expressed as follows:

$$[R_1] = \begin{bmatrix} R_{11} \\ R_{21} \\ R_{31} \\ R_{41} \\ R_{51} \\ R_{61} \\ R_{71} \\ R_{81} \\ R_{91} \\ R_{101} \\ R_{111} \end{bmatrix} = \begin{bmatrix} \beta_1 K_1 - \lambda_{d_1} m_{11} \\ \beta_2 K_2 - \lambda_{d_2} m_{21} \\ \beta_3 K_3 - \lambda_{d_3} m_{31} \\ \beta_4 K_4 - \lambda_{d_4} m_{41} \\ \beta_5 K_5 - \lambda_{d_5} m_{51} \\ \beta_6 K_6 - \lambda_{d_6} m_{61} \\ \beta_7 K_7 - \lambda_{d_7} m_{71} \\ \beta_8 K_8 - \lambda_{d_8} m_{81} \\ \beta_9 K_9 - \lambda_{d_9} m_{91} \\ \beta_{10} K_{10} - \lambda_{d_{10}} m_{101} \\ \beta_{11} K_{11} - \lambda_{d_{11}} m_{111} \end{bmatrix} \begin{bmatrix} \Phi_{d_{11}} \\ \Phi_{d_{21}} \\ \Phi_{d_{31}} \\ \Phi_{d_{41}} \\ \Phi_{d_{51}} \\ \Phi_{d_{61}} \\ \Phi_{d_{71}} \\ \Phi_{d_{81}} \\ \Phi_{d_{91}} \\ \Phi_{d_{101}} \\ \Phi_{d_{111}} \end{bmatrix} \tag{10}$$

The objective function with regard to the residual force matrix R and the reduction parameter β_i can be written as $f(\beta_1, \beta_2, \ldots, \beta_n) = \sqrt{R_1^2 + R_2^2 + \ldots + R_m^2}$. Finally, the objective function is expressed as:

$$F = \frac{1}{1 + f(\beta_1, \beta_2, \ldots, \beta_n)} \tag{11}$$

Assuming that damage leads to a loss of stiffness without affecting the mass, 2-bay truss structure analysis using residual force method employs the residual force method and several optimization methods to analyze structural damage. This approach utilizes modal vibration data, such as eigenvalues and eigenvectors. The modal analysis-based method offers advantages:

- Modal parameters are determined solely by the mechanical properties of the structures, making them less sensitive to environmental changes.
- It can save the time and expense associated with damage monitoring.

The objective function for optimization methods should be with respect to parameters associated with the physical characteristics and condition of the structure. Each parameter represents the decrease in stiffness of a specific element. The objective function includes a vector of residual forces that is expressed with regard to the stiffness matrix of the damaged structure.

The experiments on the 2-bay truss structure with eigenvalues were conducted using a total of four test cases:

1. 50% Stiffness Reduction at Element 7
2. 20% Stiffness Reduction at Element 10

 doi:10.20944/preprints202407.0858.v1

3. Multiple Damage: 30% Stiffness Reduction at Element 3, 20% Stiffness Reduction at Element 8

The cost function used in the verification for the damage detection using the bio-inspired optimization is defined as follows with reference to Equation (9):

$$\mathcal{L}(\beta) = \sqrt{\sum_{i=1}^{m} \left\| -\lambda_{i,i}[M]p_i + \sum_{j=1}^{n} \beta_j [K]_j p_i \right\|^2} \tag{12}$$

$$0 \leq \beta_j \leq 1 \quad \text{for} \quad j = 1, 2, \ldots, n \tag{13}$$

The Equation (12) is the cost function used for the optimization problem concerning a 2-bay truss structure. Here, m represents the number of mode shapes, indicating the shapes obtained from three different vibrations applied. n denotes the number of elements constituting the 2-bay structure, which is set to 11 as shown in the Figure 2. The parameter β, which we aim to predict, is set as a list with a length of n, where each element in the list is a real number ranging between 0 and 1.

These test cases were designed to evaluate the effectiveness of the optimization methods in detecting and quantifying structural damages. By analyzing the results from these diverse scenarios, the robustness and accuracy of the Residual Force Method (RFM) can be thoroughly assessed. To apply the Residual Force Method (RFM) to a 2-bay truss structure, various optimization methods have been employed. GA, PSO, SLnO and CRO can be examples of methods. Each of these optimization techniques offers unique advantages in minimizing the residual forces and adjusting the structural parameters to enhance the accuracy of the finite element model. By utilizing these methods, the efficiency and precision of the RFM process are significantly improved, leading to more reliable predictions of the structural behavior under various loading conditions.

The experiments applied four optimization methods to the four test cases of the 2-bay truss structure. The damage evaluation of the algorithm is expressed as Figure 3, and all algorithms perform well, resulting in similar performance graphs for all algorithms. Representatively, the performance graph for SLnO is illustrated as Figure 3. The performance of each optimization method was evaluated based on the average error calculated for each element of the truss structure. The average error across all elements served as the performance metric. The average errors observed for each optimization method were as follows:

Table 1. Average errors for different optimization methods. The table shows the performance of each method in terms of average error percentage.

Optimization algorithm	Average Error (%)
GA	0.0001
PSO	0.0006
SLnO	0.0126
CRO	0.5064

(a) 2nd case **(b)** 3rd case **(c)** 4th case

Figure 3. This is the result of the diffness reduction in different elements predicted through optimization algorithm. (**a**) applied 50% stiffness reduction to the seventh element, and (**b**) applied 20% stiffness reduction to the tenth element. (**c**) applied 30% and 20% stiffness reduction to the third and eighth elements, respectively.

 doi:10.20944/preprints202407.0858.v1

The results indicate that optimization methods such as GA and PSO exhibited lower average errors compared to SLnO and CRO. This can be attributed to the relatively simple nature of the data and computations involved, allowing the simpler GA and PSO algorithms to perform better. The results suggest that applying bio-inspired optimization techniques can be applied to estimate and to detect the damage in the structures.

4. Vision Based Structural Health Monitoring System Using Phase-Based Motion Magnification

4.1. Fundamentals of Phase-Based Motion Magnification

Phase-based motion magnification is an algorithm that identifies and amplifies motion that is difficult to detect in video. By using complex stable pyramid filters [15,23], the local phase changes can be modified to amplify the phase while maintaining the amplifiers, making the motion of the structure more visible on the video. The complex steerable pyramid decomposes the input image into a local spatial phase and a local spatial amplitude depending on the location, scale, and orientation of the space. The basis functions of the complex steerable pyramid filter are Gabor wavelets and sinusoid windowed by a Gaussian envelope to estimate local motions in a specific direction [15]. The phase-based motion magnetization algorithm decomposes the input image into a partial spatial amplitude and phase part through a complex stable pyramid. The process of phase-based motion magnification is shown in Figure 4. By setting a specific frequency band, the operational deflection shapes of the vibrating structure can be measured. A larger value of the magnification factor indicates larger motions in the video; however, the magnification value should not exceed a certain critical value to prevent distortion and noise amplification.

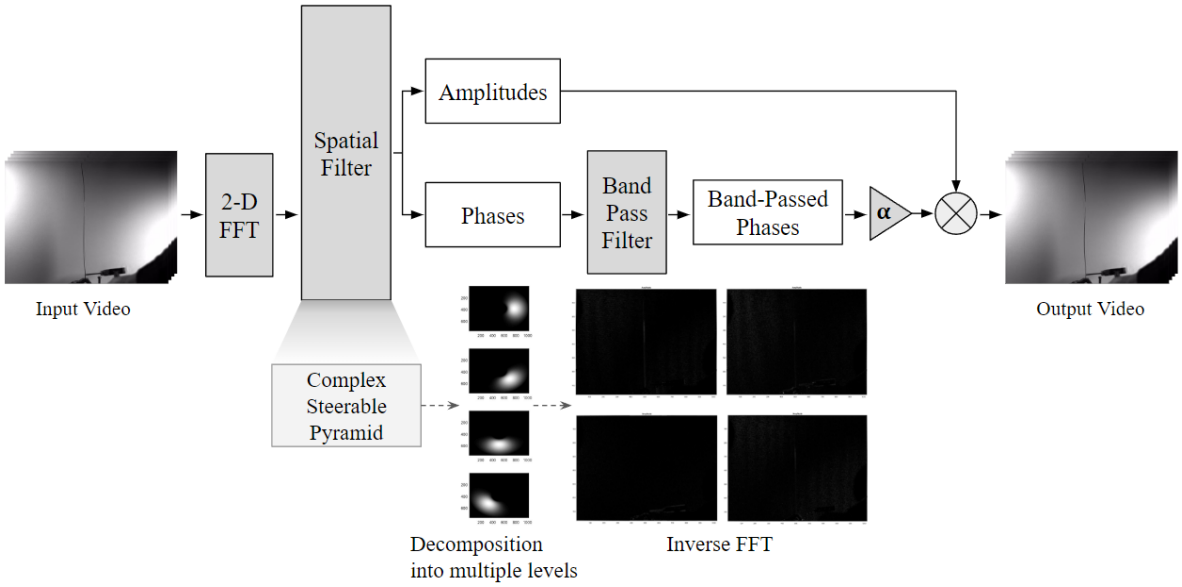

Figure 4. An architecture that represents an algorithm for converting data into vision-based. This process includes motion manipulation techniques α.

4.2. Extraction of the Natural Frequency Using the Vision-Based System

To verify the proposed vision-based motion magnification using phase-based method, the natural frequencies of undamaged and damaged cantilever beams were measured. The dynamic response of the cantilever beam was taken by 1,000 FPS Photron SA 3 high-speed camera. For the verification of measuring the natural frequencies of the undamaged and damaged cantilever beam, a Laser Doppler Velocimeter (LDV) was used as illustrated in Figure 5. For the experiment, four different types of the cantilever beams are used as follows:

1. Undamaged beam: 255mm x 25mm x 1mm

 doi:10.20944/preprints202407.0858.v1

2. Undamaged beam: 300mm x 25mm x 1mm
3. Damaged beam: 255mm x 25mm x 1mm; damaged at 55mm from the fixed end with 0.3mm depth and 1.5mm width
4. Damaged beam: 300mm x 25mm x 1mm; damaged at 99mm from the fixed end with 0.3mm depth and 1.5mm width

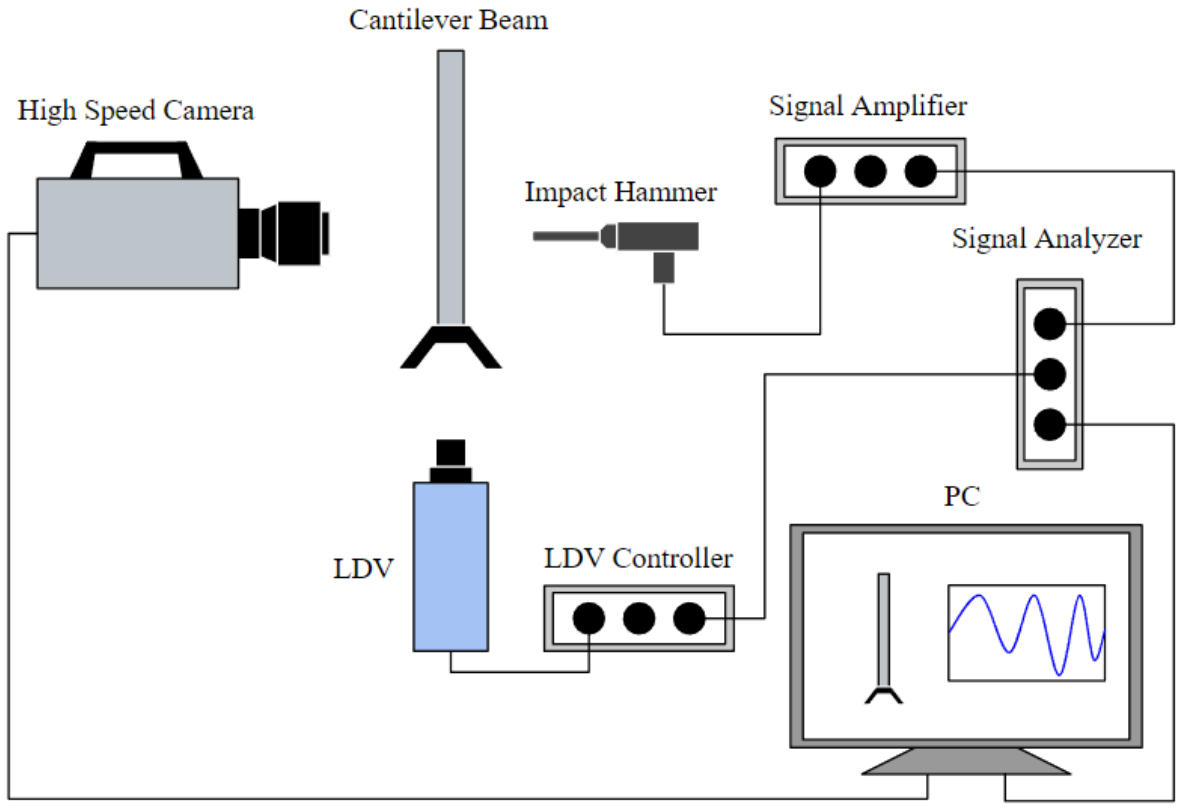

Figure 5. Experimental setting for data acquisition.

The natural frequencies of the first three modes are measured by the proposed vision-based monitoring system using phase-based motion magnification method. A comparison measurements of the natural frequencies of the undamaged cantilever beams obtained by the proposed vision-based monitoring system and LDV is shown in Table 2. The Table 3 shows damaged cantilever beams obtained by the proposed vision-based monitoring system and LDV. As Adams et al. [24] proved that a damage reduces the natural frequency, and as Tables 2 and 3 show the proposed vision-based system is practical for frequency-based structural damage detection. The natural frequencies of damaged cantilever beams measured by the vision-based system are shown in Figure 6.

Table 2. Comparison of measured natural frequencies of undamaged cantilever beams obtained by LDV and the proposed vision-based monitoring system [7]

Undamaged Cantilever Beam	Mode Number	Natural Freq. By LDV	Natural Freq. By Vision System	Error
255mm x 25mm x 1mm	1st	12.50 Hz	12.58 Hz	0.64
255mm x 25mm x 1mm	2nd	79.38 Hz	78.48 Hz	1.13
255mm x 25mm x 1mm	3rd	222.8 Hz	221.4 Hz	0.63
300 x 25mm x 1mm	1st	9.00 Hz	8.81 Hz	2.11
300 x 25mm x 1mm	2nd	57.25 Hz	57.14 Hz	0.19
300 x 25mm x 1mm	3rd	160.9 Hz	162.2 Hz	0.81

 doi:10.20944/preprints202407.0858.v1

Table 3. Comparison of measured natural frequencies of damaged cantilever beams obtained by LDV and the proposed vision-based monitoring system [7]

Damaged Cantilever Beam	Mode Number	Natural Freq. By LDV	Natural Freq. By Vision System	Error
255mm x 25mm x 1mm	1st	12.50 Hz	11.93 Hz	4.56
255mm x 25mm x 1mm	2nd	79.25 Hz	78.09 Hz	1.46
255mm x 25mm x 1mm	3rd	221.8 Hz	220.9 Hz	0.41
300 x 25mm x 1mm	1st	8.75 Hz	8.20 Hz	6.29
300 x 25mm x 1mm	2nd	55.75 Hz	56.66 Hz	1.63
300 x 25mm x 1mm	3rd	156.0 Hz	160.8 Hz	3.08

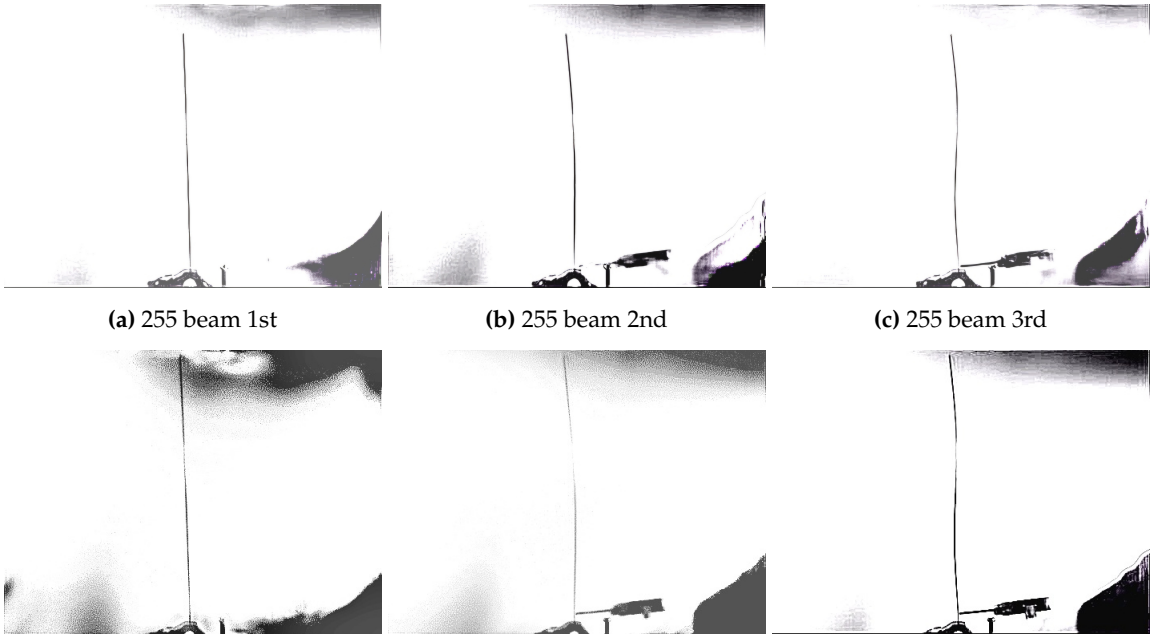

(a) 255 beam 1st **(b)** 255 beam 2nd **(c)** 255 beam 3rd

(d) 300 beam 1st **(e)** 300 beam 2nd **(f)** 300 beam 3rd

Figure 6. Extracted first three mode shapes of two damaged cantilever beams by magnified video: (**a**) estimated first mode shape of 255 mm beam, (**b**) estimated second mode shape of 255 mm, (**c**) estimated third mode shape of 255 mm beam, (**d**) estimated first mode shape of 300 mm beam, (**e**) estimated second mode shape of 300 mm beam, and (**f**) estimated third mode shape of 300 mm beam.

5. Estimation of Damage Detection in Beam Structure Using Natural Frequency and Rotational Spring Method

Rizos et al. [25] have represented a damage as rotational spring in modal analysis for a cantilever beam having a rectangular cross-section as illustrated in Figure 7. From the damage energy function, Diamarogonas and Paipetis [26] defined the rotational spring constant K in the vicinity of the damaged section of the cantilever beam when a lateral damage of uniform depth exists.

Preprints.org (www.preprints.org) | NOT PEER-REVIEWED | Posted: 10 July 2024 doi:10.20944/preprints202407.0858.v1

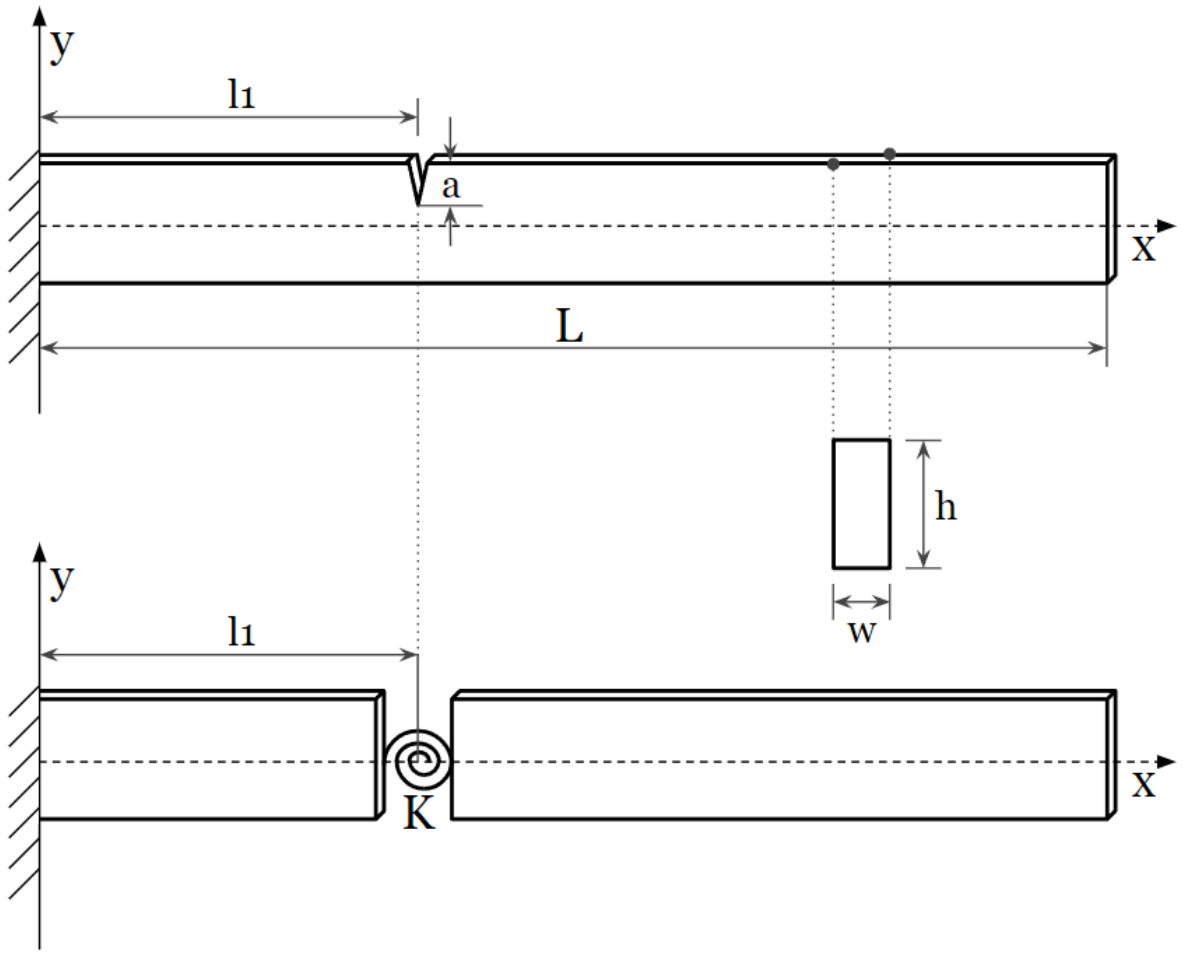

Figure 7. Cantilever beam with damage with representation of the damage as rotational spring

The damage energy function $j\left(\frac{a}{h}\right)$ describes the movement of the beam due to its geometry and material properties and is expressed as the following equation:

$$\begin{aligned} j\left(\frac{a}{h}\right) = 1.8624\left(\frac{a}{h}\right)^2 - 3.95\left(\frac{a}{h}\right)^3 + 16.375\left(\frac{a}{h}\right)^4 - 37.226\left(\frac{a}{h}\right)^5 \\ + 76.81\left(\frac{a}{h}\right)^6 - 126.9\left(\frac{a}{h}\right)^7 + 172\left(\frac{a}{h}\right)^8 - 143.97\left(\frac{a}{h}\right)^9 + 66.56\left(\frac{a}{h}\right)^{10} \end{aligned} \tag{14}$$

where $\frac{a}{h}$ is the aspect ratio of the crack depth a to the height of the beam's cross-section h. The stiffness factor K_u and the parameter λ are defined by the following equations:

$$K_u = \frac{EI}{6(1-\nu^2)h}\frac{1}{j\left(\frac{a}{h}\right)} \tag{15}$$

$$\lambda = \left(\frac{w^2 \rho A L^4}{EI}\right)^{1/4} \tag{16}$$

where E is the Young's modulus, I is the second moment of area, ν is the Poisson's ratio, h is the height of the beam's cross-section, $j\left(\frac{a}{h}\right)$ is the function describing the movement of the beam as defined Equation (14), w is the angular frequency defined as $2\pi f$ where f is the frequency in hertz (Hz). ρ is the material's density, A is the cross-sectional area, and L is the length of the beam. The stiffness factor K_u represents the beam's resistance to deformation, factoring in the material's elasticity, geometric properties, and the $j\left(\frac{a}{h}\right)$ function. The parameter λ incorporates the effects of material density, cross-sectional area, and other factors influencing the beam's dynamic response.

 doi:10.20944/preprints202407.0858.v1

To estimate the damage of the cantilever beam, the determinant of the matrix M, which is essential for the analysis of the cantilever beam, must be calculated. The matrix M is defined as:

$$M = \begin{bmatrix} M_{11} & M_{12} \\ M_{21} & M_{22} \end{bmatrix} \tag{17}$$

where each sub-matrix represents different aspects of the beam's dynamic response, incorporating both hyperbolic and trigonometric functions to model the beam's behavior accurately.

$$M_{11} = \begin{bmatrix} 1 & 0 & 1 & 0 \\ 0 & 1 & 0 & 1 \\ \cosh\left(\frac{\lambda l_1}{L}\right) & \sinh\left(\frac{\lambda l_1}{L}\right) & \cos\left(\frac{\lambda l_1}{L}\right) & \sin\left(\frac{\lambda l_1}{L}\right) \\ \sinh\left(\frac{\lambda l_1}{L}\right) & \cosh\left(\frac{\lambda l_1}{L}\right) & \sin\left(\frac{\lambda l_1}{L}\right) & -\cos\left(\frac{\lambda l_1}{L}\right) \end{bmatrix}$$

$$M_{12} = \begin{bmatrix} 0 & 0 & 0 & 0 \\ 0 & 0 & 0 & 0 \\ \cosh\left(\frac{\lambda l_1}{L}\right) & \sinh\left(\frac{\lambda l_1}{L}\right) & \cos\left(\frac{\lambda l_1}{L}\right) & \sin\left(\frac{\lambda l_1}{L}\right) \\ \sinh\left(\frac{\lambda l_1}{L}\right) & \cosh\left(\frac{\lambda l_1}{L}\right) & \sin\left(\frac{\lambda l_1}{L}\right) & \cos\left(\frac{\lambda l_1}{L}\right) \end{bmatrix}$$

$$M_{21} = \begin{bmatrix} \cosh\left(\frac{\lambda l_1}{L}\right) & \sinh\left(\frac{\lambda l_1}{L}\right) & \cos\left(\frac{\lambda l_1}{L}\right) & \sin\left(\frac{\lambda l_1}{L}\right) \\ 0 & 0 & 0 & 0 \\ 0 & 0 & 0 & 0 \\ \frac{k_u L}{EI\lambda}\sinh\left(\frac{\lambda l_1}{L}\right) + \cosh\left(\frac{\lambda l_1}{L}\right) & \frac{k_u L}{EI\lambda}\cosh\left(\frac{\lambda l_1}{L}\right) + \sinh\left(\frac{\lambda l_1}{L}\right) & -\frac{k_u L}{EI\lambda}\sin\left(\frac{\lambda l_1}{L}\right) - \cos\left(\frac{\lambda l_1}{L}\right) & -\frac{k_u L}{EI\lambda}\cos\left(\frac{\lambda l_1}{L}\right) + \sin\left(\frac{\lambda l_1}{L}\right) \end{bmatrix}$$

$$M_{22} = \begin{bmatrix} \cosh\left(\frac{\lambda l_1}{L}\right) & \sinh\left(\frac{\lambda l_1}{L}\right) & \cos\left(\frac{\lambda l_1}{L}\right) & \sin\left(\frac{\lambda l_1}{L}\right) \\ \cosh(\lambda) & \sinh(\lambda) & \cos(\lambda) & \sin(\lambda) \\ \sinh(\lambda) & \cosh(\lambda) & \sin(\lambda) & \cos(\lambda) \\ \frac{k_u L}{EI\lambda}\sinh\left(\frac{\lambda l_1}{L}\right) & \frac{k_u L}{EI\lambda}\cosh\left(\frac{\lambda l_1}{L}\right) & \frac{k_u L}{EI\lambda}\sin\left(\frac{\lambda l_1}{L}\right) & \frac{k_u L}{EI\lambda}\cosh\left(\frac{\lambda l_1}{L}\right) \end{bmatrix} \tag{18}$$

6. Damage Detection Using Bio-Inspired Optimization Methods

This section represents the results of damage detection performance on the cantilever beams using bio-inspired optimization algorithms. This study investigates the application of four bio-inspired optimization algorithms for the damage detection in the cantilever beams using natural frequencies obtained from proposed vision-based monitoring system. As bio-inspired Optimization algorithms, four different methods are used: GA, PSO, SLnO, and CRO. The experiments were conducted on two damaged cantilever beams of 255 mm and 300 mm, comparing the results obtained from GA in our previous research [7] with the newly conducted results of PSO, SLnO, and CRO in this study.

$$\mathcal{L}(l_1, a) = \sum_{i=1}^{n} (f_i^{\text{real}} - f_i^{\text{estim}})^2 \tag{19}$$

$$0 \leq l_1 \leq L \quad \text{and} \quad 0 \leq a \leq h \tag{20}$$

The error is calculated using Equation (19). In this cost function, f^{real} represents the natural frequency of the beam with the actual crack, and f^{estim} denotes the natural frequency predicted by the algorithms. The variable n is the number of natural frequency employed, which is set to 3 in this experiment. Equation (20) is a constraint of the optimization problem for cantilever beams, where L and h are the total length and height of the cantilever beams, respectively. The l_1 and a to be estimated are illustrated in Figure 7.

6.1. Damage Detection for 255mm Cantilever Beam

Experiments were conducted on the cantilever beam with dimensions $L = 255$ mm, $h = 1$ mm, and $w = 2.5$ mm. The actual damage was located at $l_1 = 54$ mm to 55.5 mm with a depth $a = 0.3$ mm. The results for each optimization algorithm are represented in Table 4.

 doi:10.20944/preprints202407.0858.v1

Table 4. Damage detection results for the 255 mm cantilever beam.

Algorithm	Estimated l_1 (mm)	Error (%)	Estimated a (mm)	Error (%)
GA [7]	52.72	2.37	0.350	16.67
PSO	48.617	11.07	0.26934	12.79
SLnO	53.676	0.60	0.30328	1.08
CRO	51.549	4.75	0.30129	0.43

6.2. Damage Detection for 300mm Cantilever Beam

Experiments were conducted on a cantilever beam with dimensions $L = 300$ mm, $h = 1$ mm, and $w = 2.5$ mm. The actual crack was located at $l_1 = 99$ mm to 100.5 mm with a depth $a = 0.3$ mm. The results for each optimization algorithm are shown in Table 5.

Table 5. Damage detection results for the 300 mm cantilever beam.

Algorithm	Estimated l_1 (mm)	Error (%)	Estimated a (mm)	Error (%)
GA [7]	87.3	11.8	0.392	30.67
PSO	98.794	0.21	0.37316	19.60
SLnO	101.23	0.72	0.27240	10.13
CRO	100.78	0.28	0.29661	1.14

6.3. Result Analysis

This study demonstrated the bio-inspired optimization algorithms can effectively detect damage in the cantilever beams. The learning curves of optimizers implemented for each cantilever beam are summarized in Figure 8. As a result of the evaluated algorithms, the swarm-based optimization algorithm, CRO, achieved the lowest average error with 1.65% among other optimization algorithms which demonstrated the best performance as shown in Table 6. It indicates that CRO is highly effective in accurately detecting damage for both crack location and depth in cantilever beams, outperforming other bio-inspired algorithms.

Table 6. Average errors for different optimization methods. This table shows the performance of each method in terms of average error percentage.

Optimization algorithm	Average Error (%)
GA [7]	15.38
PSO	10.92
SLnO	3.13
CRO	1.65

 doi:10.20944/preprints202407.0858.v1

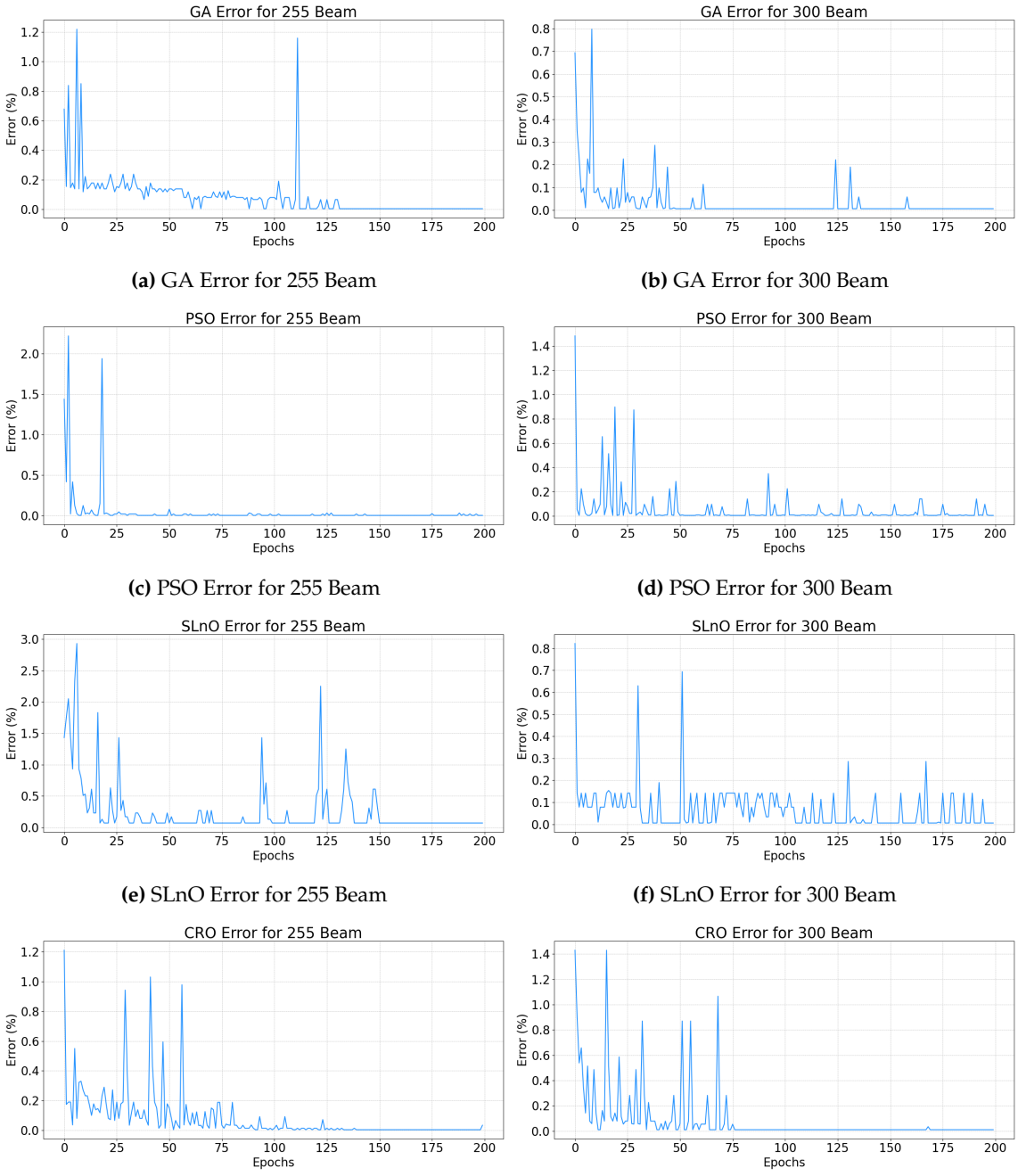

(a) GA Error for 255 Beam **(b)** GA Error for 300 Beam

(c) PSO Error for 255 Beam **(d)** PSO Error for 300 Beam

(e) SLnO Error for 255 Beam **(f)** SLnO Error for 300 Beam

(g) CRO Error for 255 Beam **(h)** CRO Error for 300 Beam

Figure 8. The learning curve of optimizers implemented for each cantilever beam.

7. Conclusions

This work is an extended work of our previous research [7] to improve the natural frequency based damage detection accuracy of the cantilever beam using vision-based monitoring system. In order to verify the performance of bio-inspired optimization methods on the Structural Health Monitoring (SHM), the damage detection on the two-bay truss structure was performed. The proposed vision-based monitoring system was used for the damage detection on the cantilever beams. The natural frequencies of four different cantilever beams were measured to verify the proposed vision-based monitoring system using phase-based magnification method. Then, the obtained natural frequencies were compared to the natural frequencies obtained from LDV measurements. After the verification of the vision-based monitoring system, the measured natural frequencies were used for the damage detection. The estimation of the damage location and depth in the cantilever beams were formulated

as a global optimization problem. The four different bio-inspired optimization methods are used (GA, PSO, SLnO, and CRO). As the result, the swarm-based optimization algorithm, CRO has the most accurate estimation rate on the damage detection.

Further research on several aspects of this work can improve the proposed vision-based monitoring system, which has great potential for the SHM field.

Future work will attempt not only to extend the vision-based monitoring system to extract mode shapes of the structure, but also to expand the proposed method to complex structures such as contained coupled mode shapes with Deep Learning approach such as Vision Transformer and LSTM based methods to analysis sequential data.

Author Contributions: Conceptualization, M.J., J.K. and A.J.C.; methodology, M.J. and J.K.; software, M.J.; validation, M.J., J.K. and A.J.C.; formal analysis, M.J.; investigation, M.J.; resources, A.J.C.; data curation, M.J., J.K. and A.J.C.; writing—original draft preparation, M.J.; writing—review and editing, A.J.C.; visualization, J.K.; supervision, A.J.C.; project administration, A.J.C.; funding acquisition, A.J.C. All authors have read and agreed to the published version of the manuscript.

Funding: This research was funded by the Gachon University Research Fund of 2024 (GCU- 202400520001).

Institutional Review Board Statement: Not Applicable.

Informed Consent Statement: Not Applicable.

Data Availability Statement: Data will be made available on request.

Conflicts of Interest: The authors declare no conflicts of interest.

References

1. Yan, K.; Zhang, Y.; Yan, Y.; Xu, C.; Zhang, S. Fault diagnosis method of sensors in building structural health monitoring system based on communication load optimization. *Smart Mater. Struct.* **2020**, *29*, 105034. doi:10.1088/0964-1726/29/10/105034.
2. Hassani, S.; Dackermann, U. A Systematic Review of Optimization Algorithms for Structural Health Monitoring and Optimal Sensor Placement. *Sensors* **2023**, *23*, 1050.
3. Sun, H.; Büyüköztürk, O. Optimal sensor placement in structural health monitoring using discrete optimization. *Smart Mater. Struct.* **2015**, *24*, 125034. doi:10.1088/0964-1726/24/12/125034.
4. Guo, H.Y.; Zhang, L.; Zhang, L.L.; Zhou, J.X. Optimal placement of sensors for structural health monitoring using improved genetic algorithms. *Smart Mater. Struct.* **2004**, *13*, 528. doi:10.1088/0964-1726/13/3/011.
5. Eltouny, K.; Gomaa, M.; Liang, X. Unsupervised Learning Methods for Data-Driven Vibration-Based Structural Health Monitoring: A Review. *Sensors* **2023**, *23*, 3290.
6. Shabbir, K.; Umair, M.; Sim, S.-H.; Ali, U.; Noureldin, M. Estimation of Prediction Intervals for Performance Assessment of Building Using Machine Learning. *Sensors* **2024**, 24, 4218.
7. Choi, A.J.; Han, J.-H. Frequency-based damage detection in cantilever beam using vision-based monitoring system with motion magnification technique. *J. Intell. Mater. Syst. Struct.* **2018**, *29*, 3923-3936. doi:10.1177/1045389X18790245.
8. Zhou, L.; Huang, P.; Chi, S.; Li, M.; Zhou, H.; Yu, H.; Cao, H.; Chen, K. Structural health monitoring of offshore wind power structures based on genetic algorithm optimization and uncertain analytic hierarchy process. *Renewable Energy* **2020**, *147*, 1783-1795. doi:10.1016/j.renene.2019.09.116.
9. Barontini, A.; Masciotta, M.-G.; Ramos, L.F.; Amado-Mendes, P.; Lourenço, P.B. An overview on nature-inspired optimization algorithms for Structural Health Monitoring of historical buildings. *Journal of Cultural Heritage* **2021**. doi:10.1016/j.culher.2021.01.007.
10. Das, S.; Saha, P.; Satapathy, S.C.; Jena, J.J. Social group optimization algorithm for civil engineering structural health monitoring. *Appl. Soft Comput.* **2020**, *96*, 1651-1670. doi:10.1016/j.asoc.2020.106491.
11. Loh, K.J.; Ryu, D.; Lee, B.M. Bio-inspired Sensors for Structural Health Monitoring. In *Bio-inspired Sensors for Structural Health Monitoring*; Springer: New York, NY, USA, **2020**; Chapter 11.
12. Vakil-Baghmisheh, M.-T.; Peimani, M.; Sadeghi, M.H.; Ettefagh, M.M. Crack detection in beam-like structures using genetic algorithms. *Appl. Soft Comput.* **2008**, *8*, 1150–1160.
13. Boonlong, K. Vibration-Based Damage Detection in Beams by Cooperative Coevolutionary Genetic Algorithm. *Adv. Mech. Eng.* **2014**, *6*, 1–12.

14. Chen, J.G.; Wadhwa, N.; Cha, Y.J.; Durand, F.; Freeman, W.T.; Buyukozturk, O. Modal identification of simple structures with high-speed video using motion magnification. *J. Sound Vib.* **2015**, *345*, 58–71.
15. Yang, Y.; Dorn, C.; Mancini, T.; Talken, Z.; Kenyon, G.; Farrar, C.; Mascarenas, D. Blind identification of full-field vibration modes from video measurements with phase-based video motion magnification. *Mech. Syst. Signal Process.* **2017**, *85*, 567–590.
16. Poozesh, P.; Sarrafi, A.; Mao, Z.; Avitabile, P.; Niezrecki, C. Feasibility of extracting operating shapes using phase-based motion magnification technique and stereo-photogrammetry. *J. Sound Vib.* **2017**, *407*, 350–366.
17. Mitchell, M. *An Introduction to Genetic Algorithms*; MIT Press: Cambridge, MA, USA, **1998**.
18. Algedir, A.A.; Refai, H.H. Energy Efficiency Optimization and Dynamic Mode Selection Algorithms for D2D Communication Under HetNet in Downlink Reuse. *IEEE Access* **2020**, *8*, 95251–95265.
19. Kennedy, J.; Eberhart, R. Particle swarm optimization. In *Proceedings of the ICNN'95 - International Conference on Neural Networks*, Perth, WA, Australia, 27 November–1 December **1995**; Volume 4, pp. 1942–1948.
20. Heppner, F.; Grenander, U. A stochastic nonlinear model for coordinated bird flocks. In *The Ubiquity of Chaos*; Krasner, S., Ed.; AAAS Publications: Washington, DC, USA, **1990**.
21. Masadeh, R.; Mahafzah, B.A.; Sharieh, A. Sea Lion Optimization Algorithm. *Int. J. Adv. Comput. Sci. Appl.* **2019**, *10*, 1–10.
22. Salcedo-Sanz, S.; Del Ser, J.; Landa-Torres, I.; Gil-López, S.; Portilla-Figueras, J.A. The Coral Reefs Optimization Algorithm: A Novel Metaheuristic for Efficiently Solving Optimization Problems. *The Scientific World Journal* **2014**, 2014, 15 pages. doi:10.1155/2014/739768.
23. Wadhwa, N.; Rubinstein, M.; Durand, F.; Freeman, W.T. Phase-based video motion processing. *ACM Trans. Graph.* **2013**, *32*, 1–10.
24. Adams, R. D.; Walton D.; Flitcroft, J. E. Short, D. Vibration testing as a nondestructive test tool for composite materials. *J. Compos. Mater* **1975**, *13*, 161–175.
25. Rizos, P. F.; Aspragathos, N. A.; Dimarogonas, A. D. Identification of Crack Location and Magnitude in a Cantilever Beam From the Vibration Modes. *J. Sound Vib.* **1990**, *138*, 381–388.
26. Diamarogonas, A. D.; Paipetis, S. A. *Analytic Methods in Rotor Dynamics*, 2nd ed.; Springer: New York, USA, **1983**.